


# Testing galaxy formation models with the stellar mass-halo mass relations for star-forming and quiescent galaxies

KAI WANG <sup>1,2,3,\*</sup> AND YINGJIE PENG<sup>1,4,†</sup>

<sup>1</sup>*Kavli Institute for Astronomy and Astrophysics, Peking University, Beijing 100871, China*

<sup>2</sup>*Institute for Computational Cosmology, Department of Physics, Durham University, South Road, Durham, DH1 3LE, UK*

<sup>3</sup>*Centre for Extragalactic Astronomy, Department of Physics, Durham University, South Road, Durham DH1 3LE, UK*

<sup>4</sup>*Department of Astronomy, School of Physics, Peking University, Beijing 100871, China*

## ABSTRACT

The tight relationship between the stellar mass and halo mass of galaxies is one of the most fundamental scaling relations in galaxy formation and evolution. It has become a critical constraint for galaxy formation models. Over the past decade, growing evidence has convincingly shown that the stellar mass-halo mass relations (SHMRs) for star-forming and quiescent central galaxies differ significantly: at a given stellar mass, the average host halo mass of quiescent centrals is more massive than that of the star-forming centrals. Despite the importance of this feature, its scientific implications have been largely overlooked and inadequately discussed. In this work, we demonstrate that the semi-analytical model L-GALAXIES successfully reproduces these observational results, whereas three state-of-the-art hydrodynamic galaxy formation simulations (TNG, Illustris, and EAGLE) do not. Consequently, in L-GALAXIES, star-forming central galaxies are more efficient at converting baryons into stars than quiescent central galaxies at a given halo mass, while the other models predict similar efficiencies for both populations. Further analysis reveals that these fundamental discrepancies stem from distinct evolutionary paths on the stellar mass-halo mass plane. We show that the observed SHMRs for star-forming and quiescent galaxies support galaxy formation models in which quenching only weakly correlates with halo assembly histories, and in which the stellar mass of star-forming galaxies can increase significantly since cosmic noon. In contrast, models in which quenching strongly prefers to happen in early-formed halos are disfavored. Additionally, we find that galaxy downsizing is present in L-GALAXIES and TNG, but absent in Illustris and EAGLE.

*Keywords:* method: statistical - galaxies: evolution - galaxies: formation - galaxies: halos - galaxies: groups: general

## 1. INTRODUCTION

Galaxies are formed and evolved within dark matter halos, where baryons are accreted by dark matter halos to fuel star formation, and the converted stellar mass is limited by the total available baryons, which scales with halo mass. Regarding the intimate interplay between star formation and halo growth, a tight scaling relation between the stellar mass of galaxies and the host halo mass, named as the stellar mass-halo mass relation, is expected (Cooray & Sheth 2002; Baugh 2006; Mo et al. 2010; Wechsler & Tinker 2018). In fact, numerous efforts in the last decades have been devoted to measur-

ing SHMR in observation, based on various techniques, like gravitational lensing (Mandelbaum et al. 2016; Bilicki et al. 2021; Zhang et al. 2022), satellite kinematics (More et al. 2011; Li et al. 2012, 2013; Zhang et al. 2022), dynamical modelling (Lapi et al. 2018; Posti et al. 2019; Posti & Fall 2021; Di Teodoro et al. 2023), etc. The most remarkable finding is that all different methods deliver highly convergent scaling relation between stellar mass and halo mass, despite different assumptions on which they are based.

The observed SHMR tells us that the stellar mass to halo mass ratio, which is the efficiency of converting baryons into stars, is low overall, which means that the star formation process is quite inefficient. In addition, the efficiency is suppressed at the low- and high-mass end, which suggests at least two mechanisms to sup-

\* KW: wkcosmology@gmail.com

† YP: yjpeng@pku.edu.cn

press the star formation efficiencies, operating in low-mass and high-mass halos separately (Yang et al. 2003, 2012; Conroy & Wechsler 2009; Behroozi et al. 2010; Moster et al. 2013). This result provokes numerous observational and theoretical studies on the feedback effect from stellar wind, supernovae explosion, and the accretion of super-massive black holes in galaxy center, and their impact on the global galaxy properties, such as the star formation rate (Kauffmann et al. 1993; Kang et al. 2005; Croton et al. 2006). It also leads to the proposal of other mechanisms to suppress stellar conversion efficiency, which is exemplified by the inefficient gas cooling in massive dark matter halos (Dekel et al. 2009).

Regarding the impactful findings elicited by measuring and understanding the SHMR for the general population of galaxies, several studies have initiated the measurement of SHMRs for different populations of galaxies, such as star-forming galaxies versus quiescent galaxies, and they converged to the same conclusion: at fixed stellar mass, quiescent/red central galaxies on average occupy more massive dark matter halos than star-forming/blue central galaxies. In other words, *at fixed stellar mass, star-forming/blue central galaxies are more efficient in converting their available baryons into stars* (e.g. More et al. 2011; Mandelbaum et al. 2016; Zu & Mandelbaum 2016; Posti et al. 2019; Posti & Fall 2021; Zhang et al. 2022). However, the scientific implications of these observational results have been inadequately discussed in literature. In this work, we start with the comparison between observational results and galaxy formation models, pointing out that most of the state-of-the-art galaxy formation models fail to reproduce the observational result, and discuss its scientific implications on the relationship between star formation histories and halo growth histories, as well as stringent constraints that can be put on galaxy formation models.

This paper is structured as follows: §2 introduces observational results on the SHMR of star-forming and quiescent galaxies and galaxy formation models. §3 presents the comparison between observations and models. §4 discusses the implication on the modeling of galaxy formation and evolution, followed by a summary in §5. Throughout this paper, we adopt a concordance cosmology with  $\Omega_\Lambda = 0.7$ ,  $\Omega_m = 0.3$ , and  $h = 0.7$ . All logarithms are 10-based.

## 2. DATA

### 2.1. Observations

We compile observational measurements of the SHMRs for different populations of galaxies in literature and present them on the first two panels in Fig. 1 with a brief introduction presented as follows.

*Satellite kinematics*—More et al. (2011) measure the halo mass of blue and red central galaxies selected from SDSS survey using the kinematics of surround satellite galaxies. They find that red central galaxies occupy more massive halos than blue central galaxies at fixed stellar mass. Recent studies using satellite kinematics draw the same conclusion (see Zhang et al. 2022).

*Weak gravitational lensing*—Mandelbaum et al. (2016) measure the halo mass of blue and red local brightest galaxies (LBG)<sup>1</sup>, separately, using the weak gravitational lensing technique in SDSS. They found that red LBGs live in halos on average more massive than blue LBGs by 0.4-1 dex, and the significance of this difference is greater than  $3\sigma$ . Similar conclusions were drawn in subsequent studies in different surveys (e.g. Bilicki et al. 2021; Zhang et al. 2022)

*Rotation curve*—Lapi et al. (2018) compile a sample of 550 disk-dominated galaxies with rotation curve measurements, from which they can estimate their host halo mass. Posti et al. (2019) measure the halo mass of 108 spiral galaxies with HI rotation curve measurements and find that massive spiral galaxies can convert 30%-100% of their available baryons into stars, where the efficiency is much higher than that of the general population of galaxies, which are normally below 20%. Di Teodoro et al. (2023) perform the 3D kinematic modeling for 15 massive spiral galaxies in the local Universe and confirm the previous result.

*Globular cluster systems*—Posti & Fall (2021) measure the halo mass of 25 early-type galaxies based on the kinematics of their globular cluster systems, from which they find that the stellar conversion efficiency of these early-time galaxies peaks at  $M_* \approx 5 \times 10^{10} M_\odot$  and  $M_h \approx 1 \times 10^{12} M_\odot$ , in sharp contrast to the results of the late-type galaxies in their earlier work (see Posti et al. 2019).

### 2.2. Galaxy formation models

*Semi-analytical modeling*—L-GALAXIES is a semi-analytical model of galaxy formation, built on halo merger trees extracted from the Millennium N-body cosmological simulations. Galaxies are seeded within dark matter halos, and then the accreted baryons, along with the growth of dark matter halo, are used to feed star formation, once the accreted gas is sufficiently cooled down and compressed. It also models various astrophysical processes that affect global galaxy properties, such as stellar feedback, metal production, the growth and

<sup>1</sup> Local brightest galaxies are selected as those galaxies with no brighter neighbors within 1 Mpc and  $\pm 1000$ km/s.

feedback from the super-massive black hole located at the center of each galaxy, the merging of galaxies and subsequent starbursts, and others. The free parameters in the model recipes are constrained by the stellar mass function and the fraction of passive galaxies across the redshift range from 0 to 3. We refer to [Henriques et al. \(2015\)](#) for more details (see also [Guo et al. 2011](#)).

*Hydrodynamical simulations*—**IllustrisTNG** (hereafter **TNG**; [Weinberger et al. 2017](#); [Naiman et al. 2018](#); [Marinacci et al. 2018](#); [Nelson et al. 2018](#); [Pillepich et al. 2018a,b](#); [Nelson et al. 2019](#)), **Illustris** ([Vogelsberger et al. 2014a,b](#); [Genel et al. 2014](#); [Sijacki et al. 2015](#); [Nelson et al. 2015](#)), and **EAGLE** ([Schaye et al. 2015](#); [McAlpine et al. 2016](#); [The EAGLE team 2017](#)) are three state-of-the-art cosmological hydrodynamical galaxy formation simulations, in which dark matter, stars, gas, and super-massive black hole are represented by discrete particles, whose evolution should be governed by fundamental physical laws. Nevertheless, given the limited computational power, these simulations still need empirical recipes to model physical processes that are below the resolution limit but have an impact on larger scales. These processes are exemplified by star formation, stellar feedback, and the growth and feedback of super-massive black holes, which are also the major factors that differentiate different simulations. We refer to specific papers on these simulations for more details.

For all simulations, dark matter halos are identified using the Friends-of-Friends (FoF) algorithm ([Davis et al. 1985](#)), and subhalos are identified using the SUBFIND algorithm ([Springel et al. 2001](#)) in each FoF halo. Across redshift snapshots, merger trees are constructed using the algorithm in [Springel et al. \(2005\)](#), and the main branch is constructed by recursively selecting the progenitor subhalo with the most massive history ([De Lucia & Blaizot 2007](#)). The halo mass is defined as the total mass enclosed in a radius within which the mean density just exceeds 200 times the critical density at the given redshift. The stellar mass is defined as the recommended way in each simulation, which is the total stellar mass within 30 physical kpc in **EAGLE** and within twice the half-mass radius in **Illustris** and **TNG**. The same aperture is also applied to the calculation of star formation rate (SFR) in each simulation.

### 2.3. Separating two populations of galaxies

It is noteworthy that different studies separate galaxies into two populations based on different types of galaxy bi-modality. For instance, [Mandelbaum et al. \(2016\)](#) discriminate blue and red galaxies based on their  $g-r$  color; so do [More et al. \(2011\)](#), while [Bilicki et al. \(2021\)](#) uses the  $u-g$  color. [Lapi et al. \(2018\)](#) and [Posti](#)

& [Fall \(2021\)](#) separate early-type galaxies from late-type galaxies based on their morphology (see also [Posti et al. 2019](#)). Meanwhile, we use the current star formation rate to classify star-forming and quiescent galaxies (see also [Zhang et al. 2022](#)). Nevertheless, due to the intimate relationship among these bi-modalities (see [Blanton & Moustakas 2009](#)), these different separation criteria deliver similar results (see one example in [Zhang et al. 2022](#)), regarding even larger uncertainties in constraining the halo mass.

## 3. RESULT

### 3.1. Comparing models to observations

There have been numerous efforts devoted to measuring the SHMRs of star-forming and quiescent central galaxies in our local Universe, and a compilation of these observational results is shown in Fig 1. The top-left panel shows the measurements based on stacking systems with similar stellar mass together to measure their halo properties, which is exemplified by weak gravitational lensing (e.g. [Mandelbaum et al. 2016](#); [Bilicki et al. 2021](#); [Zhang et al. 2022](#)) and satellite kinematics (e.g. [More et al. 2011](#); [Zhang et al. 2022](#)). All these results, despite their inherent systematics, agree on the qualitative conclusion that red and quiescent central galaxies tend to live in more massive dark matter halos than their blue and star-forming counterparts at fixed stellar mass. The same trend can also be inferred from the top-middle panel, where the halo mass is measured for each individual galaxy by modeling either the rotation curves or the globular cluster systems (e.g. [Lapi et al. 2018](#); [Posti et al. 2019](#); [Posti & Fall 2021](#); [Di Teodoro et al. 2023](#)). Moreover, we can see that those late-type galaxies follow a single power-law relation on the stellar mass-halo mass plane (see also [Posti et al. 2019](#)), and this differs from the SHMR for all central galaxies, whose slope steepens at the massive end.

The remaining four panels show the results from four state-of-the-art galaxy formation models, including one semi-analytical model (**L-GALAXIES**) and three cosmological hydrodynamical galaxy formation simulations (**TNG**, **Illustris**, and **EAGLE**). To begin with, the hatched region in all panels shows the 16<sup>th</sup> – 84<sup>th</sup> quantiles of halo mass as a function of stellar mass in **L-GALAXIES** for reference. Here one can see that the low/high-mass end is dominated by star-forming/quiescent galaxies, and all observations and simulations agree on this scaling relation for the general population of galaxies quite well. In fact, all these galaxy formation models are tuned to match the observed galaxy stellar mass function. Meanwhile, the halo mass function is mostly determined by the cos-

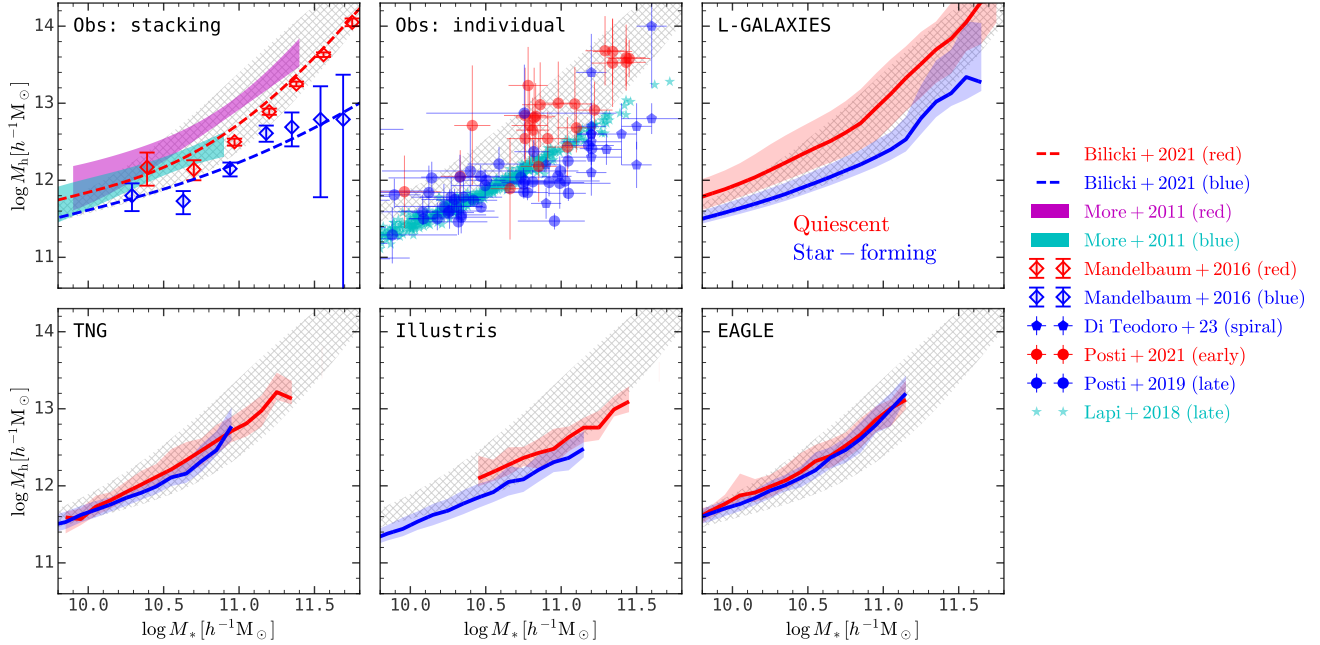


**Figure 1.** The stellar mass-halo mass relation for star-forming and quiescent central galaxies. The top-left panel is for observational results from weak gravitational lensing (see Mandelbaum et al. 2016; Bilicki et al. 2021) and satellite kinematics (see More et al. 2011). The top-middle panel is for the measurement of individual galaxies, where the halo mass is constrained by rotation curves (Lapi et al. 2018; Posti et al. 2019; Di Teodoro et al. 2023) and globular cluster systems (Posti & Fall 2021). The remaining four panels are for the results of four different galaxy formation models: L-GALAXIES, TNG, Illustris, and EAGLE. The hatched region in all panels shows the 16<sup>th</sup> – 84<sup>th</sup> quantiles of halo mass as a function of stellar mass for all central galaxies in L-GALAXIES for reference. This figure demonstrates that star-forming and quiescent central galaxies follow different stellar mass-halo mass scaling relations, and L-GALAXIES can reproduce this trend while the other three hydrodynamical galaxy formation simulations fail to do so.

mological parameters. Therefore, as long as the model generates more massive galaxies in more massive halos, which is also the heuristic assumption in the sub-halo abundance matching model (see Mo et al. 1999; Vale & Ostriker 2004), they can deliver the same stellar mass-halo mass relation. Hence, we rely on the SHMRs for different populations of galaxies to further discriminate different galaxy formation models. Secondly, at fixed stellar mass, L-GALAXIES gives a large dispersion of halo mass, while the SHMRs in all three hydrodynamical simulations are very tight, leaving no room for a difference in halo mass for star-forming and quiescent central galaxies. Last but not least, L-GALAXIES predicts that quiescent central galaxies live in more massive halos than star-forming central galaxies at fixed stellar mass, in consistency with observational results, while all three hydrodynamical simulations predict indistinguishable SHMRs for these two populations (see Marasco et al. 2020; Zhang et al. 2022), except for a minor difference in Illustris.

### 3.2. Switching the axes

Observational results based on stacking methods, like weak gravitational lensing and satellite kinematics, only give the average halo mass at fixed stellar mass. However, stellar mass itself is subject to many uncertain baryonic physics, so, if attempting to analyze galaxy formation processes with fixed descendant stellar mass, we also need to model the exchange of galaxies between different descendant stellar mass bins, which could be very complicated. On the other hand, halo mass is much more resistant to these baryonic processes, at least in the mass range of our interests in this work, so the analysis could be greatly simplified if we could switch the axes and study the stellar mass difference at fixed halo mass for star-forming and quiescent central galaxies.

At the first sight of the top-left panel in Fig. 1, one might naively infer that star-forming galaxies should have higher stellar mass than quiescent galaxies at fixed halo mass. However, different claims, where star-forming galaxies are equally massive or less massive than quiescent galaxies at a given halo mass, could also reproduce the observational results (see Zu & Mandelbaum 2016; Behroozi et al. 2019; Moster et al. 2020; Tinker 2021, for examples). Thanks to the measurements of

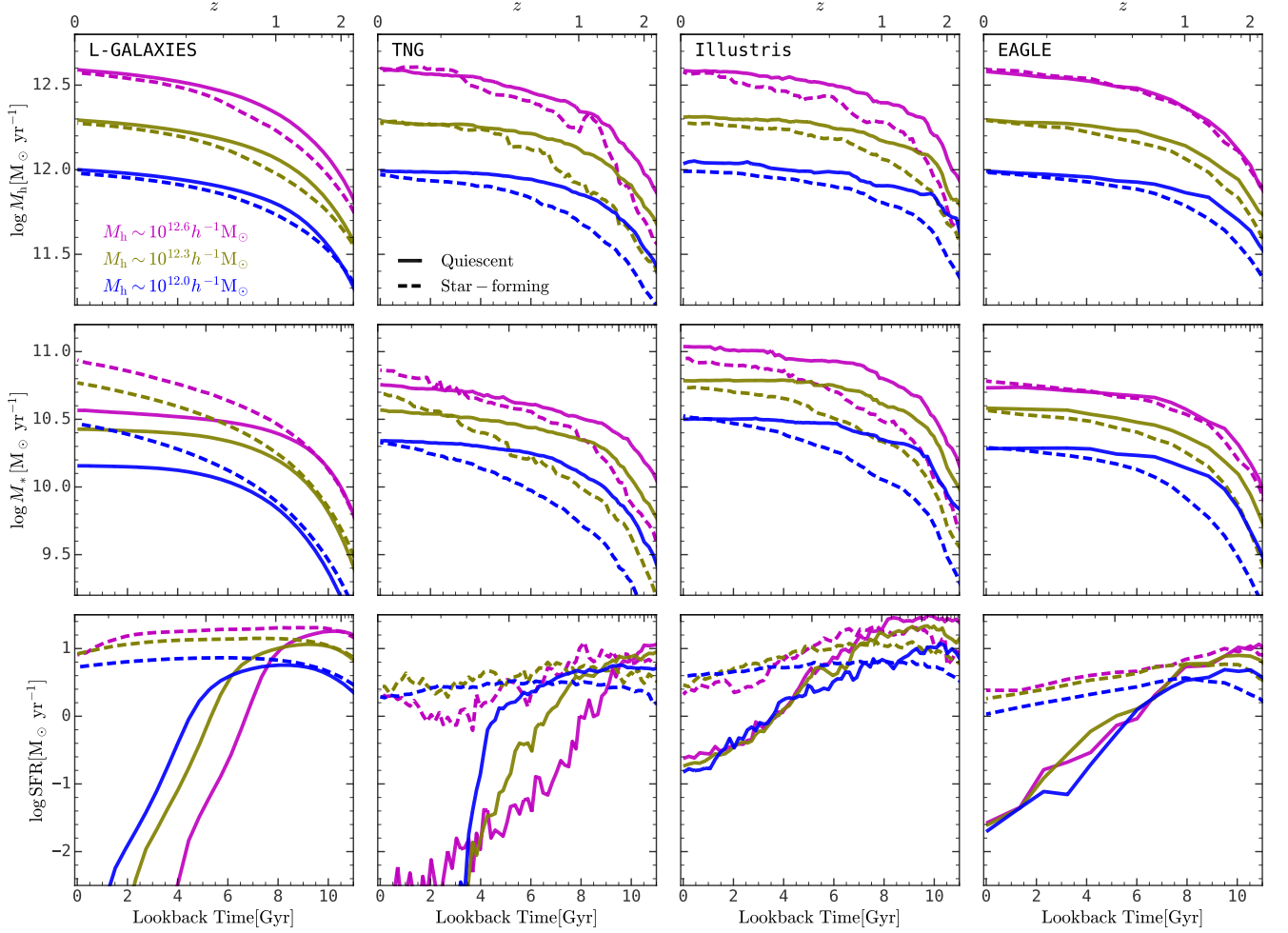


**Figure 2.** The redshift evolution of halo mass (top panels), progenitor stellar mass (middle panels), and star formation rate (bottom panels) for quiescent (solid) and star-forming (dashed) central galaxies selected at  $z = 0$  in four different galaxy formation models. Here central galaxies are binned into three  $z = 0$  halo mass bins and each bin has a width of 0.2 dex.

stellar mass and halo mass for individual systems (see the top-middle panel in Fig. 1), we can directly inspect the stellar mass difference between star-forming and quiescent galaxies at fixed halo mass, and we do see that star-forming central galaxies have higher stellar mass than quiescent central galaxies with similar halo mass (see Lapi et al. 2018; Posti et al. 2019; Posti & Fall 2021; Di Teodoro et al. 2023). In fact, similar conclusions are obtained by conditional stellar mass function (see Figure 5 in Rodríguez-Puebla et al. 2015) and halo occupation distribution (see Figure 19 in Xu et al. 2018)<sup>2</sup> modelling extended to incorporate with galaxy color, and the mod-

eling of satellite kinematics (see Figure 8 in More et al. 2011).

### 3.3. Relating star formation history to halo assembly history

After switching the axe, we concluded that, at fixed halo mass, star-forming central galaxies have higher stellar mass than quiescent central galaxies. We then proceed to study the evolution of these two populations of galaxies conditioned on their  $z = 0$  halo mass, aiming to figure out the underlying reason that L-GALAXIES can reproduce observational results, while all three hydrodynamical galaxy formation models fail to do so. Before we start, it is noteworthy that all current galaxy formation models are calibrated against observational summary statistics, such as the stellar mass function, so that they can agree on the SHMR for the general population, as one can see in Fig. 1. Therefore, we are only inter-

<sup>2</sup> We note that Xu et al. (2018) built their model using the luminosity of galaxies instead of stellar mass, and the color dependence of stellar mass-to-light ratio will exaggerate the halo mass-to-light ratio different for blue and red central galaxies, so caution must be taken when comparing with their results.

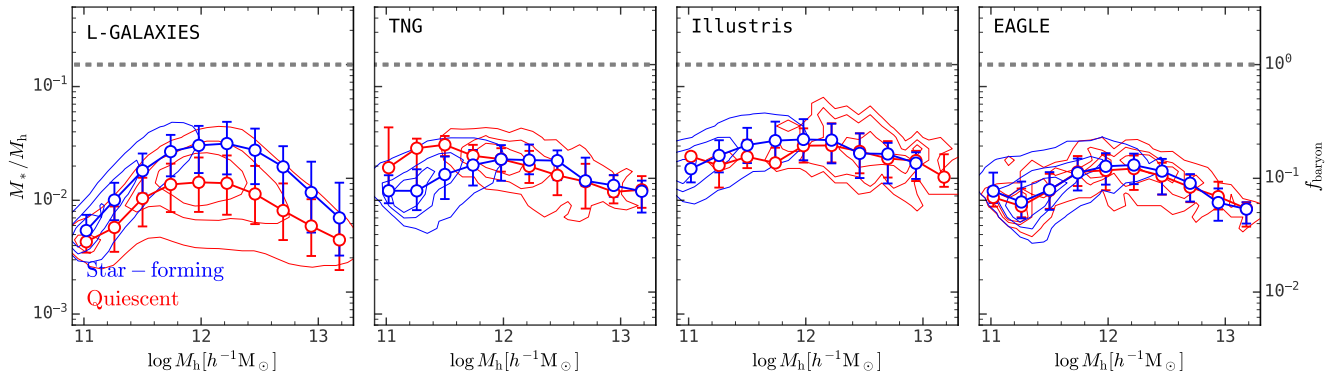


**Figure 3.** The central stellar mass-to-halo mass ratio as a function of halo mass for four different galaxy formation models at  $z = 0$ . The background contour lines enclose 30%, 60%, and 90% star-forming and quiescent central galaxies in blue and red, respectively. The error bars show the median and 16<sup>th</sup> – 84<sup>th</sup> quantiles of the ratio in each halo mass bin. The y-axis on the right side shows  $f_{\text{baryon}} = \Omega_m/\Omega_b \times M_*/M_h$ . This figure shows that, in L-GALAXIES, star-forming central galaxies are more efficient in converting baryons into stars than quiescent central galaxies, while other models give similar efficiencies for these two populations.

ested in the stellar mass difference of star-forming and quiescent central galaxies at fixed halo mass at  $z = 0$ .

Fig. 2 shows the evolution of halo mass, stellar mass, and star formation rate along the main branch of the galaxy merger tree as a function of lookback time for star-forming and quiescent central galaxies at fixed descendant halo mass. We start from the halo growth history, where all galaxy formation models predict that quiescent central galaxies prefer to live in early-formed halos. However, the difference in the halo growth history for star-forming and quiescent central galaxies is significant in three hydrodynamical simulations, but marginal in L-GALAXIES. In other words, all three hydrodynamical simulations predict strong correlations between the halo growth history and the descendant star formation status, while L-GALAXIES gives a weak correlation.

We then move on to the stellar mass growth history, as shown in the middle panels in Fig. 2, and we find significant differences among different galaxy formation models. In L-GALAXIES, star-forming and quiescent galaxies have almost identical stellar mass history initially, when their progenitor galaxies were both star-forming. Then, for whatever reason<sup>3</sup>, some galaxies are quenched, and their stellar mass history flattened, while the remaining galaxies were still actively making new stars to increase their stellar mass. Consequently, when evolved to  $z = 0$ , star-forming galaxies end up with stellar mass 0.3 – 0.4 dex higher than those quiescent galaxies on average. This result is consistent with the picture pro-

posed in Peng et al. (2012) to explain the halo mass difference for red and blue central galaxies in observation (see also Man et al. 2019).

For TNG and its precedence, Illustris, as shown on the panels in the middle two columns, the halos that host quiescent descendant central galaxies are assembled much earlier than those with star-forming central galaxies. Then, the progenitor stellar mass of quiescent central galaxies grows much faster than that of star-forming central galaxies at the early stage, benefiting from their more massive progenitor halos and more available baryons at high- $z$ . Then, when these galaxies are quenched, their stellar mass growth is suppressed and the advantage in stellar mass accumulated at early times will be gradually consumed. Eventually, the stellar mass of quiescent galaxies become very close to that of star-forming galaxies, or could even be surpassed by the latter, as one can see in TNG. For EAGLE, galaxies and their dark matter halos evolve similarly.

A similar conclusion could be obtained from reading the evolution of SFR for star-forming and quiescent galaxies, as shown on the bottom panels of Fig. 2. In L-GALAXIES, the SFR histories<sup>4</sup> were identical for these two populations, then, after a while, the progenitor SFR of quiescent galaxies damped, while the remaining galaxies are still actively forming new stars. For all three hydrodynamical galaxy formation simulations, the progenitors of quiescent galaxies have much higher SFR than those of star-forming galaxies at the initial stage, and

<sup>3</sup> In L-GALAXIES, massive central galaxies are quenched by the feedback from accreting super-massive black holes in the galaxy center, since it will heat the cold gas content, making it unavailable for subsequent star formation.

<sup>4</sup> This SFR history is different from the star formation history we usually refer to in spectral energy distribution fitting, in which case all progenitor branches are considered, and here we only include the main branch.

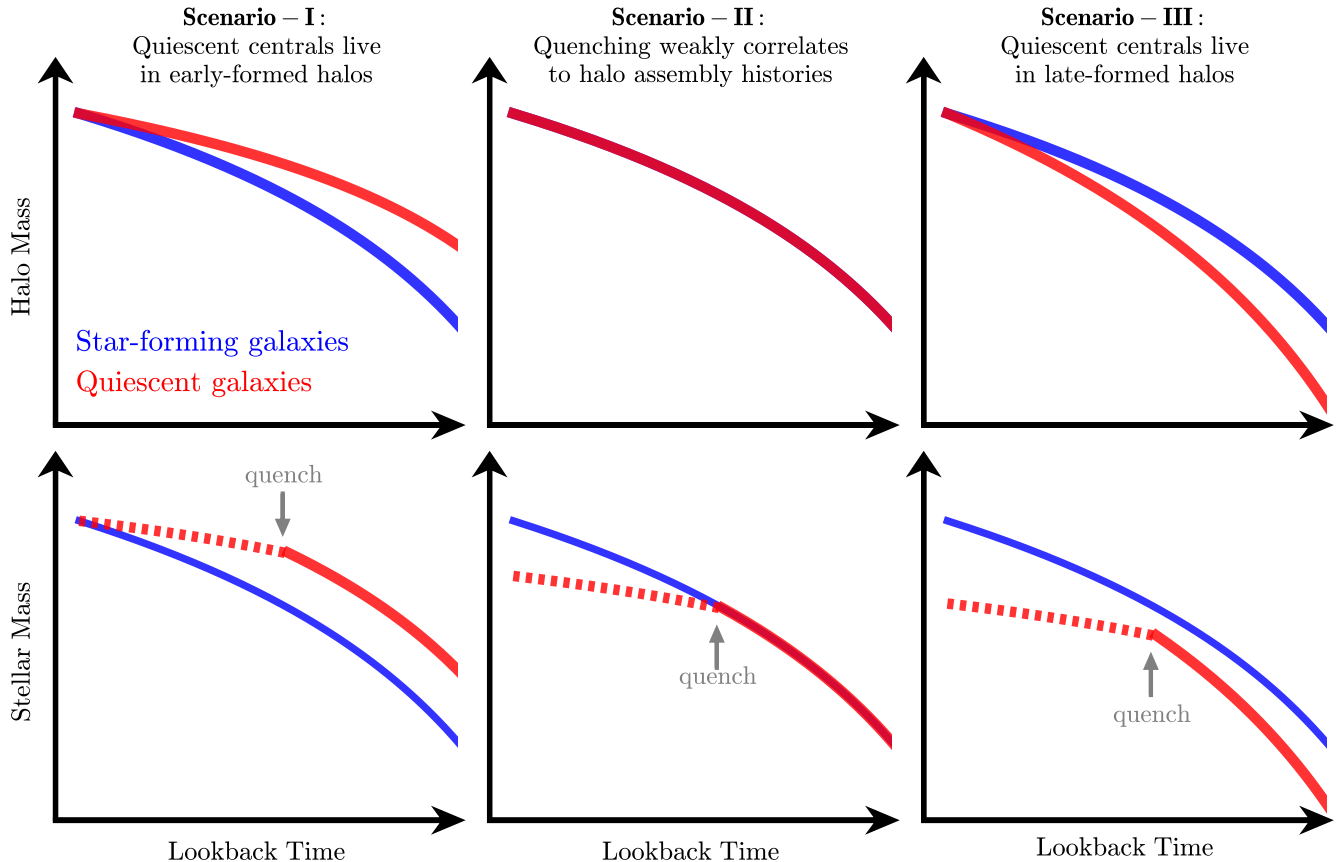


**Figure 4.** Illustration of the redshift evolution of halo mass and stellar mass for star-forming (blue) and quiescent (red) descendant galaxies at  $z = 0$ . In **Scenario-I** (left panels), quiescent central galaxies at  $z = 0$  prefer to live in early-formed halos. In this case, the progenitor galaxies of quiescent central galaxies were initially more massive since their progenitor halos are more massive and most of the central galaxies at high redshifts are star-forming. However, once these galaxies are quenched, their stellar growth will be suppressed and, consequently, these two populations of galaxies end up with similar stellar masses. In **Scenario-II** (middle panels), quiescent central galaxies live in halos with similar assembly histories as star-forming central galaxies. In this case, the progenitor galaxies of these two populations of galaxies have similar stellar mass at early times. Then, once some galaxies are quenched, their stellar mass growth will be suppressed and end up with lower stellar mass compared with their star-forming counterparts, which trend is consistent with observational results. In **Scenario-III** (right panels), quiescent central galaxies live in late-formed halos. In this case, the progenitor galaxies of quiescent central galaxies not only possess lower stellar mass at early times, but also are suppressed in their stellar mass growth after quenching, compared with their star-forming counterparts. Consequently, the stellar mass difference becomes larger.

the difference in their stellar mass was compensated by the opposite SFR difference at late times. Eventually, these two populations of galaxies have similar stellar mass-to-halo mass ratios.

The cautious reader may have noticed that, in *EAGLE*, star-forming and quiescent galaxies have similar halo mass growth history, but end up with similar descendant stellar mass nonetheless. We found central galaxies in these massive halos in *EAGLE* have lower SFR than those in the other two simulations, and especially so when compared to *L-GALAXIES*. Consequently, those star-forming galaxies cannot surpass their quiescent counterparts too much in terms of stellar mass, even

if the latter is quenched at some stage. Therefore, to reproduce observational results, another required condition is that star-forming galaxies must grow their stellar mass significantly after cosmic noon.

In addition, we found that a clear dependence of galaxy quenching time on the descendant halo mass in *L-GALAXIES*, where central galaxies end up in massive halos are quenched earlier than those that end up in less massive halos. This is a manifestation of galaxy downsizing (Cowie et al. 1996; Fontanot et al. 2009, e.g.), which is also present in *TNG*, but absent in the remaining two hydrodynamical galaxy formation simulations.

### 3.4. *Stellar conversion efficiency*

We have seen that L-GALAXIES gives distinct stellar mass growth history for star-forming and quiescent galaxies, compared with three hydrodynamical galaxy formation models, and it explains that L-GALAXIES can reproduce observational SHMRs for different populations of galaxies while others fail to do so. Another way to understand this result is through the efficiency of converting baryons into stars, as Fig. 3 presents the stellar mass-to-halo mass ratio for star-forming and quiescent central galaxies as a function of halo mass for four galaxy formation models. Despite the resemblance of their overall shape, which peaks around  $10^{12}h^{-1}M_{\odot}$  and is suppressed at both low-mass and high-mass ends, star-forming galaxies have higher ratios than quiescent galaxies by  $\approx 0.3$  dex in L-GALAXIES, while all three hydrodynamical galaxy formation simulations give almost identical ratios for these two populations of galaxies. In other words, star-forming galaxies are much more efficient in converting baryons into stars than quiescent galaxies in L-GALAXIES, while, in the other three models, the stellar conversion efficiencies are close to each other for these two populations of galaxies. It seems that these hydrodynamical simulations, despite their distinct subgrid physics in modeling stellar feedback and AGN feedback, can self-regulate the evolution of galaxies (Booth & Schaye 2009; Schaye et al. 2010, 2015), so that these two populations of galaxies end up with similar stellar mass conversion efficiency.

## 4. DISCUSSION

### 4.1. *How to relate star formation history to halo growth history?*

How to relate the growth of galaxies to their host dark matter halos plays an essential role in modeling galaxy formation and evolution. In fact, many empirical models attempt to directly link these two types of histories to populate galaxies into dark matter halos/subhalos (e.g. Conroy & Wechsler 2009; Behroozi et al. 2010; Lu et al. 2014; Mo et al. 2024). Here we want to show that the observed SHMRs for star-forming and quiescent galaxies can put a stringent constraint on these models. Before we start, it is noteworthy that the SHMR for the general population of galaxies is well-constrained in observations and well-converged among models, and here we only intend to discuss the difference between star-forming and quiescent central galaxies at a given halo mass at  $z = 0$ , which is also all we are concerned about in this study.

As illustrated in Fig. 4, there are three different scenarios. In **Scenario-I**, quiescent galaxies live in early-formed halos (see Hearin & Watson 2013; Hearin et al. 2014; Wang et al. 2023b), which is exemplified by three

hydrodynamical galaxy formation simulations in this work. At high redshift, the progenitors of quiescent galaxies grow faster since these galaxies are star-forming at early times and they have more available baryons due to more massive halos they reside in. Later on, once these galaxies are quenched at some point, their stellar mass growth will be suppressed, letting their star-forming counterparts catch up. Finally, these two populations of galaxies will end up with similar stellar mass when evolved to  $z = 0$ , as we have seen in Fig. 2 for the three hydrodynamical galaxy formation simulations.

**Scenario-II** assumes that the stellar growth history only weakly relates to the halo assembly history (e.g. Peng et al. 2012; Man et al. 2019; Lyu et al. 2023; Lyu et al. 2024), which is exemplified by L-GALAXIES. In this case, the progenitors of both star-forming and quiescent galaxies grow in a similar pace at high redshift since they are all star-forming and live in similar dark matter halos. Then, the progenitors of quiescent galaxies must be quenched prior to  $z = 0$  and, once that happens, their stellar mass growth will be suppressed and result in lower stellar mass than their star-forming counterparts, just as we have seen in Fig. 2 for L-GALAXIES. This scenario could produce the stellar mass difference between star-forming and quiescent central galaxies at fixed halo mass required by observations.

The last one, **Scenario-III**, assumes that quiescent galaxies live in late-formed halos (e.g. Cui et al. 2021; Wang et al. 2023a; Mo et al. 2024). In this case, the stellar mass of star-forming central galaxies is larger than their quiescent counterparts to a higher degree. This is because not only the stellar mass growth of quiescent galaxies was suppressed later on, but also the progenitors of quiescent galaxies have lower stellar mass than those star-forming counterparts at high redshift due to less massive progenitor halo mass and less available baryons.

It is noteworthy that **Scenario-II** and **Scenario-III** predict that low-stellar-mass central galaxies are more likely to be quenched than those with high stellar mass at fixed halo mass, which seems to be in contradictory to observational results that more massive galaxies are more quenched. However, Wang et al. (2023a) indeed found this trend in our local Universe, so it could also be true for high- $z$  Universe, which could be tested using upcoming high- $z$  galaxy surveys, like PFS (Takada et al. 2014) and MOONS (Cirasuolo et al. 2014), together with high- $z$  group finders (e.g. Wang et al. 2020; Yang et al. 2021; Li et al. 2022).

Qualitatively speaking, observational results presented in §2 support the last two scenarios, while the scenario in which quiescent central galaxies that live in



early-formed halos are strongly disfavored. We also note that further discriminating between **Scenario-II** and **Scenario-III** relies on more quantitative and more accurate observational constraints, which would come to reality with future deeper and larger galaxy surveys.

## 5. SUMMARY

The stellar mass-halo mass relation for central galaxies, as one of the most fundamental scaling relations in galaxy formation and evolution, has not only put stringent constraints on galaxy formation models, but also elicited numerous observational and theoretical work on understanding the feedback processes that regulate galaxy evolution. Regarding these impactful findings, measurements of SHMRs for different populations of galaxies have been initiated and refined in the last decade. Despite the innate systematics of different methods, all these studies drew on the same conclusion: at fixed stellar mass, red and quiescent central galaxies tend to live in more massive halos than blue and star-forming central galaxies. However, the scientific implication of this result is overlooked and inadequately discussed. In this work, we intend to initiate the discussion on testing galaxy formation models using the SHMRs for different populations of central galaxies. Our main results are summarized as follows:

1. We compare observational results, in which red/quiescent central galaxies prefer to occupy more massive halos than blue/star-forming central galaxies at fixed stellar mass, with four state-of-the-art galaxy formation models, including one semi-analytical model (**L-GALAXIES**) and three hydrodynamical simulations (**TNG**, **Illustris**, and **EAGLE**). We find that only **L-GALAXIES** is consistent with observational results, while all three hydrodynamical simulations produce almost identical SHMRs for star-forming and quiescent galaxies (see Fig. 1).
2. Based on the measurements of individual systems, we invert the axis and infer that blue and star-forming central galaxies have higher stellar mass than that of red and quiescent central galaxies at fixed halo mass.
3. We inspect the star formation history and halo growth history for halos hosting star-forming and quiescent galaxies, and find that the relationship between these two histories is very different for **L-GALAXIES** and the other three hydrodynamical

simulations. In **L-GALAXIES**, star formation histories are weakly correlated to halo growth histories, and it can successfully reproduce observational results. However, in three hydrodynamical simulations, star formation histories are strongly correlated to halo assembly histories and central galaxies in early-formed halos are more likely to be quenched when evolving to  $z = 0$ , resulting in similar stellar mass for star-forming and quiescent galaxies at  $z = 0$ , which is against observational results (see Figs. 2, 3, and 4).

4. We conclude that the observed SHMRs for star-forming and quiescent galaxies support galaxy formation models in which quenching only weakly correlates with halo assembly histories, and in which the stellar mass of star-forming galaxies can increase significantly since cosmic noon, while models in which quenching strongly prefer to happen in early-formed halos are disfavored (see Fig. 4).

This work focuses on a qualitative comparison of observational results and galaxy formation models, and it already puts stringent constraints on galaxy formation models. To fully release the constraining power of SHMRs for different populations of galaxies, more accurate observational measurements based on larger samples is demanding, especially the measurements for individual systems.

## ACKNOWLEDGEMENTS

The authors thank Yangyao Chen, Houjun Mo, and Fangzhou Jiang for their helpful comments and constructive suggestions. The authors acknowledge the Tsinghua Astrophysics High-Performance Computing platform at Tsinghua University for providing computational and data storage resources that have contributed to the research results reported within this paper. This work is supported by the National Science Foundation of China (NSFC) Grant No. 12125301, 12192220, 12192222, and the science research grants from the China Manned Space Project with NO. CMS-CSST-2021- A07.

## DATA AVAILABILITY

The data underlying this article will be shared on reasonable request to the corresponding author. The computation in this work is supported by the HPC toolkit **HIPP** (Chen & Wang 2023).

## REFERENCES

- Baugh, C. M. 2006, *Reports on Progress in Physics*, 69, 3101, doi: [10.1088/0034-4885/69/12/R02](https://doi.org/10.1088/0034-4885/69/12/R02)
- Behroozi, P., Wechsler, R. H., Hearin, A. P., & Conroy, C. 2019, *Monthly Notices of the Royal Astronomical Society*, 488, 3143, doi: [10.1093/mnras/stz1182](https://doi.org/10.1093/mnras/stz1182)
- Behroozi, P. S., Conroy, C., & Wechsler, R. H. 2010, *The Astrophysical Journal*, 717, 379, doi: [10.1088/0004-637X/717/1/379](https://doi.org/10.1088/0004-637X/717/1/379)
- Bilicki, M., Dvornik, A., Hoekstra, H., et al. 2021, *Astronomy and Astrophysics*, 653, A82, doi: [10.1051/0004-6361/202140352](https://doi.org/10.1051/0004-6361/202140352)
- Blanton, M. R., & Moustakas, J. 2009, *Annual Review of Astronomy and Astrophysics*, 47, 159, doi: [10.1146/annurev-astro-082708-101734](https://doi.org/10.1146/annurev-astro-082708-101734)
- Booth, C. M., & Schaye, J. 2009, *Monthly Notices of the Royal Astronomical Society*, 398, 53, doi: [10.1111/j.1365-2966.2009.15043.x](https://doi.org/10.1111/j.1365-2966.2009.15043.x)
- Chen, Y., & Wang, K. 2023, HIPP: HIgh-Performance Package for scientific computation, *Astrophysics Source Code Library*, record ascl:2301.030. <http://ascl.net/2301.030>
- Cirasuolo, M., Afonso, J., Carollo, M., et al. 2014, 9147, 91470N, doi: [10.1117/12.2056012](https://doi.org/10.1117/12.2056012)
- Conroy, C., & Wechsler, R. H. 2009, *The Astrophysical Journal*, 696, 620, doi: [10.1088/0004-637X/696/1/620](https://doi.org/10.1088/0004-637X/696/1/620)
- Cooray, A., & Sheth, R. 2002, *Physics Reports*, 372, 1, doi: [10.1016/S0370-1573\(02\)00276-4](https://doi.org/10.1016/S0370-1573(02)00276-4)
- Cowie, L. L., Songaila, A., Hu, E. M., & Cohen, J. G. 1996, *The Astronomical Journal*, 112, 839, doi: [10.1086/118058](https://doi.org/10.1086/118058)
- Croton, D. J., Springel, V., White, S. D. M., et al. 2006, *Monthly Notices of the Royal Astronomical Society*, 365, 11, doi: [10.1111/j.1365-2966.2005.09675.x](https://doi.org/10.1111/j.1365-2966.2005.09675.x)
- Cui, W., Davé, R., Peacock, J. A., Anglés-Alcázar, D., & Yang, X. 2021, *Nature Astronomy*, 5, 1069, doi: [10.1038/s41550-021-01404-1](https://doi.org/10.1038/s41550-021-01404-1)
- Davis, M., Efstathiou, G., Frenk, C. S., & White, S. D. M. 1985, *The Astrophysical Journal*, 292, 371, doi: [10.1086/163168](https://doi.org/10.1086/163168)
- De Lucia, G., & Blaizot, J. 2007, *Monthly Notices of the Royal Astronomical Society*, 375, 2, doi: [10.1111/j.1365-2966.2006.11287.x](https://doi.org/10.1111/j.1365-2966.2006.11287.x)
- Dekel, A., Birnboim, Y., Engel, G., et al. 2009, *Nature*, 457, 451, doi: [10.1038/nature07648](https://doi.org/10.1038/nature07648)
- Di Teodoro, E. M., Posti, L., Fall, S. M., et al. 2023, *Monthly Notices of the Royal Astronomical Society*, 518, 6340, doi: [10.1093/mnras/stac3424](https://doi.org/10.1093/mnras/stac3424)
- Fontanot, F., De Lucia, G., Monaco, P., Somerville, R. S., & Santini, P. 2009, *Monthly Notices of the Royal Astronomical Society*, 397, 1776, doi: [10.1111/j.1365-2966.2009.15058.x](https://doi.org/10.1111/j.1365-2966.2009.15058.x)
- Genel, S., Vogelsberger, M., Springel, V., et al. 2014, *Monthly Notices of the Royal Astronomical Society*, 445, 175, doi: [10.1093/mnras/stu1654](https://doi.org/10.1093/mnras/stu1654)
- Guo, Q., White, S., Boylan-Kolchin, M., et al. 2011, *Monthly Notices of the Royal Astronomical Society*, 413, 101, doi: [10.1111/j.1365-2966.2010.18114.x](https://doi.org/10.1111/j.1365-2966.2010.18114.x)
- Hearin, A. P., & Watson, D. F. 2013, *Monthly Notices of the Royal Astronomical Society*, 435, 1313, doi: [10.1093/mnras/stt1374](https://doi.org/10.1093/mnras/stt1374)
- Hearin, A. P., Watson, D. F., Becker, M. R., et al. 2014, *Monthly Notices of the Royal Astronomical Society*, 444, 729, doi: [10.1093/mnras/stu1443](https://doi.org/10.1093/mnras/stu1443)
- Henriques, B. M. B., White, S. D. M., Thomas, P. A., et al. 2015, *Monthly Notices of the Royal Astronomical Society*, 451, 2663, doi: [10.1093/mnras/stv705](https://doi.org/10.1093/mnras/stv705)
- Kang, X., Jing, Y. P., Mo, H. J., & Borner, G. 2005, *The Astrophysical Journal*, 631, 21, doi: [10.1086/432493](https://doi.org/10.1086/432493)
- Kauffmann, G., White, S. D. M., & Guiderdoni, B. 1993, *Monthly Notices of the Royal Astronomical Society*, 264, 201, doi: [10.1093/mnras/264.1.201](https://doi.org/10.1093/mnras/264.1.201)
- Lapi, A., Salucci, P., & Danese, L. 2018, *The Astrophysical Journal*, 859, 2, doi: [10.3847/1538-4357/aabf35](https://doi.org/10.3847/1538-4357/aabf35)
- Li, C., Jing, Y. P., Mao, S., et al. 2012, *The Astrophysical Journal*, 758, 50, doi: [10.1088/0004-637X/758/1/50](https://doi.org/10.1088/0004-637X/758/1/50)
- Li, C., Wang, L., & Jing, Y. P. 2013, *The Astrophysical Journal*, 762, L7, doi: [10.1088/2041-8205/762/1/L7](https://doi.org/10.1088/2041-8205/762/1/L7)
- Li, Q., Yang, X., Liu, C., et al. 2022, *The Astrophysical Journal*, 933, 9, doi: [10.3847/1538-4357/ac6e69](https://doi.org/10.3847/1538-4357/ac6e69)
- Lu, Z., Mo, H. J., Lu, Y., et al. 2014, *Monthly Notices of the Royal Astronomical Society*, 439, 1294, doi: [10.1093/mnras/stu016](https://doi.org/10.1093/mnras/stu016)
- Lyu, C., Peng, Y., Jing, Y., et al. 2023, *The Astrophysical Journal*, 959, 5, doi: [10.3847/1538-4357/ad036b](https://doi.org/10.3847/1538-4357/ad036b)
- Lyu, C., Peng, Y., Jing, Y., et al. 2024, arXiv e-prints, arXiv:2407.03409, doi: [10.48550/arXiv.2407.03409](https://doi.org/10.48550/arXiv.2407.03409)
- Man, Z.-Y., Peng, Y.-J., Shi, J.-J., et al. 2019, *The Astrophysical Journal*, 881, 74, doi: [10.3847/1538-4357/ab2ece](https://doi.org/10.3847/1538-4357/ab2ece)
- Mandelbaum, R., Wang, W., Zu, Y., et al. 2016, *Monthly Notices of the Royal Astronomical Society*, 457, 3200, doi: [10.1093/mnras/stw188](https://doi.org/10.1093/mnras/stw188)
- Marasco, A., Posti, L., Oman, K., et al. 2020, *Astronomy and Astrophysics*, 640, A70, doi: [10.1051/0004-6361/202038326](https://doi.org/10.1051/0004-6361/202038326)

- Marinacci, F., Vogelsberger, M., Pakmor, R., et al. 2018, *Monthly Notices of the Royal Astronomical Society*, 480, 5113, doi: [10.1093/mnras/sty2206](https://doi.org/10.1093/mnras/sty2206)
- McAlpine, S., Helly, J., Schaller, M., et al. 2016, *Astronomy and Computing*, 15, 72, doi: [10.1016/j.ascom.2016.02.004](https://doi.org/10.1016/j.ascom.2016.02.004)
- Mo, H., Chen, Y., & Wang, H. 2024, *Monthly Notices of the Royal Astronomical Society*, 532, 3808, doi: [10.1093/mnras/stae1727](https://doi.org/10.1093/mnras/stae1727)
- Mo, H., Van den Bosch, F., & White, S. 2010, *Galaxy Formation and Evolution* (Cambridge ; New York: Cambridge University Press)
- Mo, H. J., Mao, S., & White, S. D. M. 1999, *Monthly Notices of the Royal Astronomical Society*, 304, 175, doi: [10.1046/j.1365-8711.1999.02289.x](https://doi.org/10.1046/j.1365-8711.1999.02289.x)
- More, S., van den Bosch, F. C., Cacciato, M., et al. 2011, *Monthly Notices of the Royal Astronomical Society*, 410, 210, doi: [10.1111/j.1365-2966.2010.17436.x](https://doi.org/10.1111/j.1365-2966.2010.17436.x)
- Moster, B. P., Naab, T., & White, S. D. M. 2013, *Monthly Notices of the Royal Astronomical Society*, 428, 3121, doi: [10.1093/mnras/sts261](https://doi.org/10.1093/mnras/sts261)
- . 2020, *Monthly Notices of the Royal Astronomical Society*, 499, 4748, doi: [10.1093/mnras/staa3019](https://doi.org/10.1093/mnras/staa3019)
- Naiman, J. P., Pillepich, A., Springel, V., et al. 2018, *Monthly Notices of the Royal Astronomical Society*, 477, 1206, doi: [10.1093/mnras/sty618](https://doi.org/10.1093/mnras/sty618)
- Nelson, D., Pillepich, A., Genel, S., et al. 2015, *Astronomy and Computing*, 13, 12, doi: [10.1016/j.ascom.2015.09.003](https://doi.org/10.1016/j.ascom.2015.09.003)
- Nelson, D., Pillepich, A., Springel, V., et al. 2018, *Monthly Notices of the Royal Astronomical Society*, 475, 624, doi: [10.1093/mnras/stx3040](https://doi.org/10.1093/mnras/stx3040)
- Nelson, D., Springel, V., Pillepich, A., et al. 2019, *Computational Astrophysics and Cosmology*, 6, 2, doi: [10.1186/s40668-019-0028-x](https://doi.org/10.1186/s40668-019-0028-x)
- Peng, Y.-j., Lilly, S. J., Renzini, A., & Carollo, M. 2012, *The Astrophysical Journal*, 757, 4, doi: [10.1088/0004-637X/757/1/4](https://doi.org/10.1088/0004-637X/757/1/4)
- Pillepich, A., Springel, V., Nelson, D., et al. 2018a, *Monthly Notices of the Royal Astronomical Society*, 473, 4077, doi: [10.1093/mnras/stx2656](https://doi.org/10.1093/mnras/stx2656)
- Pillepich, A., Nelson, D., Hernquist, L., et al. 2018b, *Monthly Notices of the Royal Astronomical Society*, 475, 648, doi: [10.1093/mnras/stx3112](https://doi.org/10.1093/mnras/stx3112)
- Posti, L., & Fall, S. M. 2021, *Astronomy and Astrophysics*, 649, A119, doi: [10.1051/0004-6361/202040256](https://doi.org/10.1051/0004-6361/202040256)
- Posti, L., Fraternali, F., & Marasco, A. 2019, *Astronomy and Astrophysics*, 626, A56, doi: [10.1051/0004-6361/201935553](https://doi.org/10.1051/0004-6361/201935553)
- Rodríguez-Puebla, A., Avila-Reese, V., Yang, X., et al. 2015, *The Astrophysical Journal*, 799, 130, doi: [10.1088/0004-637X/799/2/130](https://doi.org/10.1088/0004-637X/799/2/130)
- Schaye, J., Dalla Vecchia, C., Booth, C. M., et al. 2010, *Monthly Notices of the Royal Astronomical Society*, 402, 1536, doi: [10.1111/j.1365-2966.2009.16029.x](https://doi.org/10.1111/j.1365-2966.2009.16029.x)
- Schaye, J., Crain, R. A., Bower, R. G., et al. 2015, *Monthly Notices of the Royal Astronomical Society*, 446, 521, doi: [10.1093/mnras/stu2058](https://doi.org/10.1093/mnras/stu2058)
- Sijacki, D., Vogelsberger, M., Genel, S., et al. 2015, *Monthly Notices of the Royal Astronomical Society*, 452, 575, doi: [10.1093/mnras/stv1340](https://doi.org/10.1093/mnras/stv1340)
- Springel, V., White, S. D. M., Tormen, G., & Kauffmann, G. 2001, *Monthly Notices of the Royal Astronomical Society*, 328, 726, doi: [10.1046/j.1365-8711.2001.04912.x](https://doi.org/10.1046/j.1365-8711.2001.04912.x)
- Springel, V., White, S. D. M., Jenkins, A., et al. 2005, *Nature*, 435, 629, doi: [10.1038/nature03597](https://doi.org/10.1038/nature03597)
- Takada, M., Ellis, R. S., Chiba, M., et al. 2014, *Publications of the Astronomical Society of Japan*, 66, R1, doi: [10.1093/pasj/pst019](https://doi.org/10.1093/pasj/pst019)
- The EAGLE team. 2017, arXiv:1706.09899 [astro-ph]. <http://ascl.net/1706.09899>
- Tinker, J. L. 2021, *The Astrophysical Journal*, 923, 154, doi: [10.3847/1538-4357/ac2aaa](https://doi.org/10.3847/1538-4357/ac2aaa)
- Vale, A., & Ostriker, J. P. 2004, *Monthly Notices of the Royal Astronomical Society*, 353, 189, doi: [10.1111/j.1365-2966.2004.08059.x](https://doi.org/10.1111/j.1365-2966.2004.08059.x)
- Vogelsberger, M., Genel, S., Springel, V., et al. 2014a, *Nature*, 509, 177, doi: [10.1038/nature13316](https://doi.org/10.1038/nature13316)
- . 2014b, *Monthly Notices of the Royal Astronomical Society*, 444, 1518, doi: [10.1093/mnras/stu1536](https://doi.org/10.1093/mnras/stu1536)
- Wang, K., Chen, Y., Li, Q., & Yang, X. 2023a, *Monthly Notices of the Royal Astronomical Society*, 522, 3188, doi: [10.1093/mnras/stad1175](https://doi.org/10.1093/mnras/stad1175)
- Wang, K., Mo, H., Li, C., & Chen, Y. 2023b, *Monthly Notices of the Royal Astronomical Society*, 520, 1774, doi: [10.1093/mnras/stad262](https://doi.org/10.1093/mnras/stad262)
- Wang, K., Mo, H. J., Li, C., Meng, J., & Chen, Y. 2020, *Monthly Notices of the Royal Astronomical Society*, 499, 89, doi: [10.1093/mnras/staa2816](https://doi.org/10.1093/mnras/staa2816)
- Wechsler, R. H., & Tinker, J. L. 2018, *Annual Review of Astronomy and Astrophysics*, 56, 435, doi: [10.1146/annurev-astro-081817-051756](https://doi.org/10.1146/annurev-astro-081817-051756)
- Weinberger, R., Springel, V., Hernquist, L., et al. 2017, *Monthly Notices of the Royal Astronomical Society*, 465, 3291, doi: [10.1093/mnras/stw2944](https://doi.org/10.1093/mnras/stw2944)
- Xu, H., Zheng, Z., Guo, H., et al. 2018, *Monthly Notices of the Royal Astronomical Society*, 481, 5470, doi: [10.1093/mnras/sty2615](https://doi.org/10.1093/mnras/sty2615)
- Yang, X., Mo, H. J., & van den Bosch, F. C. 2003, *Monthly Notices of the Royal Astronomical Society*, 339, 1057, doi: [10.1046/j.1365-8711.2003.06254.x](https://doi.org/10.1046/j.1365-8711.2003.06254.x)

Yang, X., Mo, H. J., van den Bosch, F. C., Zhang, Y., & Han, J. 2012, *The Astrophysical Journal*, 752, 41, doi: [10.1088/0004-637X/752/1/41](https://doi.org/10.1088/0004-637X/752/1/41)

Yang, X., Xu, H., He, M., et al. 2021, *The Astrophysical Journal*, 909, 143, doi: [10.3847/1538-4357/abddb2](https://doi.org/10.3847/1538-4357/abddb2)

Zhang, Z., Wang, H., Luo, W., et al. 2022, *Astronomy and Astrophysics*, 663, A85,

doi: [10.1051/0004-6361/202142866](https://doi.org/10.1051/0004-6361/202142866)

Zu, Y., & Mandelbaum, R. 2016, *Monthly Notices of the Royal Astronomical Society*, 457, 4360,

doi: [10.1093/mnras/stw221](https://doi.org/10.1093/mnras/stw221)